Learning increases human electroencephalographic coherence during subsequent slow sleep oscillations

Matthias Mölle*, Lisa Marshall, Steffen Gais, and Jan Born

Department of Neuroendocrinology, University of Lübeck, Ratzeburger Allee 160, Haus 23a, 23538 Lübeck, Germany

Edited by Marcus E. Raichle, Washington University School of Medicine, St. Louis, MO, and approved August 10, 2004 (received for review April 21, 2004)

Learning is assumed to induce specific changes in neuronal activity during sleep that serve the consolidation of newly acquired memories. To specify such changes, we measured electroencephalographic (EEG) coherence during performance on a declarative learning task (word pair associations) and subsequent sleep. Compared with a nonlearning control condition, learning performance was accompanied with a strong increase in coherence in several EEG frequency bands. During subsequent non-rapid eye movement sleep, coherence only marginally increased in a global analysis of EEG recordings. However, a striking and robust increase in learning-dependent coherence was found when analyses were performed time-locked to the occurrence of slow oscillations (<1 Hz). Specifically, the surface-positive half-waves of the slow oscillation resulting from widespread cortical depolarization were associated with distinctly enhanced coherence after learning in the slow-oscillatory, delta, slow-spindle, and gamma bands. The findings identify the depolarizing phase of the slow oscillations in humans as a time period particularly relevant for a reprocessing of memories in sleep.

Newly encoded memory representations are thought to remain in a fragile state and to require consolidation for long-term storage (1, 2). An extensive body of research has provided convergent evidence that sleep enhances processes of memory consolidation, presumably by an off-line "replay" of the newly encoded materials during sleep (3–5). It was first demonstrated in animal studies that patterns of hippocampal activity observed during encoding were replayed during subsequent slow-wave sleep (SWS) in rats (6–8). It has been further proposed that the spontaneous reactivation of hippocampal memory representations drives a hippocampal-neocortical transfer of the information whereby this information becomes consolidated and integrated into long-term representations residing in neocortical networks (3, 9, 10). Consistent with this view, signs were found of coherent neuronal reactivation between hippocampal and neocortical regions and within these regions during sleep after acquisition of a spatial task (11).

The replay of memories in the hippocampus and their hippocampal-neocortical transfer during SWS are assumed to be linked to a sharp wave-ripple pattern of hippocampal electroencephalographic (EEG) activity that occurs in close temporal correlation to sleep spindles in the neocortex (12, 13). In humans, intense learning of a hippocampus-dependent declarative memory task induces increased spindle activity during subsequent sleep, particularly during the first two sleep cycles in which SWS prevails (14). The occurrence of spindle and fast activity in sleep is grouped by slow oscillations (dominant frequency of 0.7–0.8 Hz) in animals as well as in humans (15–17). In the human EEG, the surface negative-going half-wave of the slow oscillation is associated with cortical disfacilitation and suppressed spindle activity (17). This negativity is followed by a pronounced increase in spindle activity during the subsequent positive-going half-wave, reflecting a widespread depolarization in cortical networks. Considering the close temporal relationship between spindle activity and hippocampal sharp wave-ripple activity, we supposed that this positive-going rebound phase in the slow oscillation represents a period of enhanced replay of information to the neocortex.

In the neocortex, oscillatory synchronization of activity in distributed cell assemblies is proposed as one general neural mechanism underlying sensory integration and information representation (18, 19). Accordingly, in humans processes of stimulus encoding and associative learning have been shown consistently to be associated with distinct increases in EEG coherence, reflecting the synchronized activity between the cortical neuron populations, contributing to the encoded representations (20–23). Here, we used measures of EEG coherence during learning of word pairs and during subsequent sleep to determine learning-dependent changes in sleep EEG that might point to a reprocessing of encoded associations. Because hippocampus-dependent memory tasks like the learning of word pairs are known to benefit particularly from SWS-rich periods of early nocturnal sleep (24, 25), we concentrated on EEG activity during non-rapid eye movement (non-REM) sleep of the first two sleep cycles after learning. Of special interest was the depolarizing positive half-wave of the slow oscillation assumed to represent a period of increased hippocampal-neocortical transfer of newly acquired representations.

Methods

Subjects and Procedures. Recordings were taken from a sample of 13 subjects (6 male and 7 female, ages 20–30, mean of 23.9 years) participating in a series of experiments exploring memory functions of sleep. All subjects were healthy, nonsmoking, native German-speaking students with regular sleep–wake rhythm during the 6 weeks before the experiments. The experiments were approved by the local ethics committee. More information on subjects, procedures, and data processing can be found in *Supporting Text*, which is published as supporting information on the PNAS web site.

After an adaptation night, subjects slept in the laboratory on two experimental nights (separated by at least 7 days) between 11:00 p.m. and 7:00 a.m. Between 9:30 and 10:30 p.m., they performed in balanced order on a "learning task" and a "nonlearning task," as described in ref. 14. On the learning task, subjects learned a paired-associate list of 336 unrelated words, arranged in 21 groups of eight pairs (e.g., factory/horse and circle/scarf). Each group of pairs was presented twice for 106 and 70 sec on the first and second run, respectively, resulting in a total learning time of 61.6 min. To induce comparable mnemonic strategies, subjects were instructed to visually imagine a relation of the two otherwise unrelated words of each pair. Recall was tested immediately after the second run of presentation and in the next morning. A cued recall testing was used; i.e., subjects were presented with the first word of each pair and had to recall the second one (no feedback was given). The

This paper was submitted directly (Track II) to the PNAS office.

Abbreviations: EEG, electroencephalography; REM, rapid eye movement; SWS, slow-wave sleep.

*To whom correspondence should be addressed. E-mail: moelle@kfg.uni-luebeck.de.

nonlearning task was designed to resemble the learning task in as many ways as possible but without the intentional learning component. On this task, subjects were instructed to count all letters containing curved lines (e.g., J, P, and U, but not W, Y, and K) on word-pair stimulus displays identical to those used for the learning task. Thus, visual input, task duration, and difficulty were equal in both conditions, but subjects had little chance to semantically process the words.

Recordings. The EEG was recorded digitally both while subjects performed the cognitive tasks and during sleep by using a SynAmps EEG amplifier (NeuroScan, Sterling, VA). EEG signals were sampled at a frequency of 500 Hz and were filtered between 0.15 and 70 Hz by using a third-order Butterworth filter (-6 dB at cutoff frequency and at least -12 dB per octave rolloff). A 50-Hz notch filter was used to reduce power frequency interference. Ag-AgCl electrodes were placed according to an extended 10–20 System (Fp1, Fp2, F3, F4, C3, C4, P3, P4, O1, O2, F7, F8, T3, T4, T5, T6, FT7, FT8, FC3, FC4, TP7, TP8, CP3, CP4, Fz, Cz, and Pz) and were referenced to linked mastoids. Additionally, horizontal and vertical eye movements and the electromyogram (chin and neck) were recorded for standard polysomnography.

Data Processing and Statistical Analysis. Each 30-sec epoch of sleep EEG was scored visually according to standard criteria (26). Sleep stages (1, 2, 3, 4, and REM sleep), awake time, and movement artifacts were scored. Stage 2 sleep corresponds to light non-REM sleep and stage 3 and 4 correspond to SWS. Scoring included a thorough visual inspection of all 27 EEG signals for movement and other artifacts during the first two sleep cycles. The EEG recorded during performance of the learning and nonlearning tasks was likewise visually inspected. All epochs with artifacts were excluded from further analysis.

For the first analysis of power and coherence, blocks of 4,096 data points ($\approx$8 sec of EEG data) were used from all artifact-free 30-sec epochs of the first and (in eight subjects) also of the second sleep cycle. Power spectra of the sleep EEG were calculated after rereferencing recordings to a common average applying fast Fourier transformations. The average number of 4,096-point blocks per subject was as follows: for stage 2 sleep, learning condition 352.6 $\pm$ 34.0 and nonlearning condition 344.9 $\pm$ 26.7; and for SWS, learning condition 227.5 $\pm$ 16.5 and nonlearning condition 239.5 $\pm$ 22.1. Individual mean fast Fourier transformations across all blocks of a condition were calculated and subjected to a five-point moving average.

Coherence spectra of EEG activity were calculated from the cross-spectral density between two EEG channels normalized by the power-spectral density of each EEG channel. For coherence calculation, the same 4,096-point blocks were used as for the power analysis. On the resulting coherence spectrum, a five-point moving average was also applied. Subsequently, mean coherences in the classical EEG bands were calculated, i.e., in the delta (1–4 Hz), theta (4–8 Hz), alpha 1 (8–10 Hz), alpha 2 (10–13 Hz), beta (15–25 Hz), and gamma (25–40 Hz) bands. Additionally, mean coherences were calculated in the frequency bands specifically characterizing sleep, i.e., in the slow-oscillation band (0.5–1.5 Hz), the slow-spindle band (stage 2 sleep, 11.5–12.5 Hz; SWS, 9.5–10.5 Hz), typically dominating over frontocortical regions, and the fast-spindle band (13.0–14.0 Hz) showing a more centroparietal distribution. The choice of these frequency bands was based on the peaks in the power spectra. Calculation of power spectra was performed separately for stage 2 sleep and SWS, and for slow-spindle activity revealed different mean peak frequencies of 11.89 $\pm$ 0.11 and 10.29 $\pm$ 0.21 Hz, respectively, during these sleep stages (see *Supporting Text*; note also that due to its frequency slow-spindle activity has been referred to as "frontal alpha" in some reports; e.g., ref. 27). The spectral peaks were clearly visible in all subjects and no other peaks were identifiable. The frequency ranges for the slow-oscillation, the slow-spindle, and the fast-spindle band were thus defined around their respective maxima.

Mean power and coherences in the delta, theta, alpha 1, alpha 2, beta, and gamma bands were also calculated from the EEG recorded during task performance before sleep. These analyses were performed in the same way as for sleep recordings on 4,096-point blocks of EEG from the first presentation of the word list (average number of blocks per subject, 174.3 $\pm$ 7.3). Before EEG coherence analysis, eye movement potentials were removed from EEG recordings by a regression method using the vertical and horizontal electrooculogram (28).

Based on previous data (17, 29), we suspected that the grouping of spindle activity by slow oscillations during non-REM sleep and SWS is linked to a learning-dependent reprocessing of newly acquired memories. On this background, it was of particular interest whether the strong rebound of spindle activity after the large negative half-wave of a slow oscillation is associated with enhanced coherence after learning. This activity was examined by a second coherence analysis, extending on an analysis (17) used for identifying slow oscillations in the human sleep EEG. After low-pass filtering of the sleep EEG signal (at Fz) within the slow-oscillation/delta band (4 Hz), the largest negative half-waves were selected by using a thresholding procedure (ref. 17; average number of half-waves per subject in stage 2 sleep, learning condition 145.5 $\pm$ 11.7 and nonlearning condition 155.7 $\pm$ 10.3; and for SWS, learning condition 141.2 $\pm$ 13.2 and nonlearning condition 148.5 $\pm$ 14.7; see *Supporting Text*). To estimate power and the coherent EEG activity in relation to the peak of the negative half-wave, blocks with 512 data points (1.024 sec) were used. On the resulting coherence spectra a three-point moving average was applied. Power and coherence were calculated in two consecutive 1-sec intervals in relation to the peak of the negative half-wave: (*i*) in the positive-going rebound interval after the peak (0–1 sec), and (*ii*) in the -1- to 0-sec interval before the peak (Fig. 2). For both intervals, mean power and coherences were calculated in the same frequency bands as described above. For further statistical analyses, power and coherence values of the 0- to 1-sec positive-going interval were standardized by subtracting respective values of the preceding -1- to 0-sec interval used as reference. To assure that results of this analysis indeed represent specific features of the positive-going interval of the slow oscillation, in a control analysis, power and coherence values were calculated in randomly distributed 1-sec intervals and values of these intervals were also standardized by subtracting respective values of immediately preceding 1-sec intervals.

Coherence analyses were calculated for 276 electrode pairs (all possible electrode pair combinations not including the sites over the longitudinal fissure, Fz, Cz, and Pz). Two-sided paired Student's t tests were used to test whether coherence for an electrode pair differed across subjects between the learning and nonlearning conditions. In coherence maps (as shown in Figs. 1 and 2), solid lines were used to indicate significantly higher coherence during learning than nonlearning. On the other hand, dashed lines indicate significantly lower coherence during learning than nonlearning conditions. For exploratory purposes, the significance level was set to $P < 0.05$ at this step of analysis. Because of the high number of Student's t tests for each coherence analysis inflating the risk of type I error, statistical inferences were subsequently based on two types of χ^2 tests: The first one was used to decide whether the number of electrode pairs with significant coherence differences is larger than the number expected per chance. The second χ^2 test was used to decide whether the number of observed electrode pairs with significantly higher coherence in the learning (than nonlearning) condition is significantly larger than the number of electrode pairs with significantly lower coherence in the learning condi-

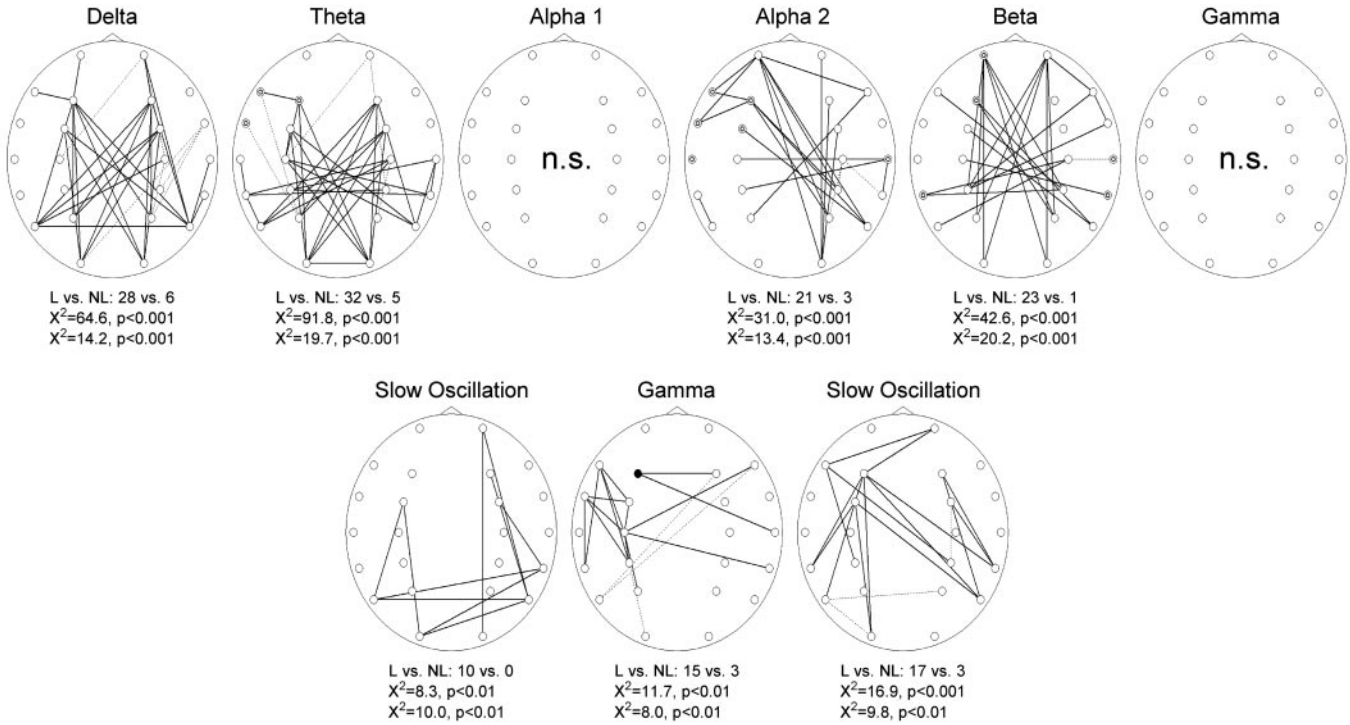

Fig. 1. Coherence maps during task performance before sleep in the classical EEG bands (*Upper*) and during stage 2 sleep and SWS, respectively, in the slow-oscillation and gamma bands, which were the only bands revealing significant coherence maps in the global analysis of sleep recordings (*Lower*). Maps indicate results for the entire subject sample ($n = 13$). Coherences were calculated for 276 pairs of electrode sites (○). Significant coherence differences ($P < 0.05$) were marked with solid lines for higher coherence during the learning condition and dashed lines for higher coherence during the nonlearning condition. Total numbers of electrode pairs with significant coherence differences between learning (L) and nonlearning (NL) and results of the χ^2 tests are indicated below each map. A map was marked NS (not significant) if the χ^2 tests failed to indicate significance. In addition, electrode sites are indicated at which power in the learning condition was significantly ($P < 0.05$) higher (●) or lower (inserted second circle) in comparison with the nonlearning condition.

tion. A coherence map was considered significant only if both χ^2 tests indicated significance ($P < 0.025$, corrected for the testing with two tests). If one of the tests failed to indicate significance or in the case that the number of electrode pairs with significant coherence differences was <10 (in which χ^2 testing is not appropriate), the maps were considered nonsignificant. Regarding the analysis of spectral power for all tests two-sided paired Student's *t* tests were used (with $P < 0.05$ considered significant).

Results

Recall Performance and Global Coherence During Learning and Sleep. Directly after learning, 71.6 ± 5.4% (mean ± SEM) of the word pairs were correctly recalled. At retrieval testing after sleep recall performance averaged 72.4 ± 5.6%.

EEG recordings during task performance before sleep revealed that learning in comparison with nonlearning induced a strong increase in EEG coherence in almost all frequency bands. This finding means that the number of electrode pairs between which EEG coherence was significantly higher during learning than nonlearning in these bands markedly exceeded the number of electrode pairs with significantly lower coherence during learning. This result held true for the delta (28 vs. 6 electrode pairs, $P < 0.001$), theta (32 vs. 5, $P < 0.001$), upper alpha (21 vs. 3, $P < 0.001$), and beta (23 vs. 1, $P < 0.001$) bands. Visual inspection of the coherence maps reveals that in the upper alpha band coherence was especially enhanced between left frontal and right parietal areas (Fig. 1).

During sleep, the number of differences in EEG coherence between the two conditions was, in general, distinctly reduced. Analysis revealed an increased coherence between electrodes after learning than nonlearning in the slow-oscillatory frequency band both during stage 2 sleep (17 vs. 3 electrode pairs for higher vs. lower coherence in the learning condition, $P < 0.01$) and SWS (10 vs. 0, $P < 0.01$; Fig. 1). In SWS, additionally, greater coherence after learning was found in the gamma band (15 vs. 3, $P < 0.01$). Other frequency bands showed no significant differences between learning and nonlearning conditions.

Complementary analyses were performed to explore differences in EEG power between the learning conditions during sleep. These analyses revealed an increased power in the upper spindle band (13.0–14.0 Hz) in the learning condition as compared with the nonlearning condition, which in stage 2 sleep was maximal at central electrode sites ($P < 0.05$, at Fz, F4, C3, Cz, C4, and P3; Fig. 3, which is published as supporting information on the PNAS web site). During SWS, it dominated over frontocortical sites ($P < 0.05$, at Fp1, Fp2, and F3), extending over this region also into the adjacent beta band ($P < 0.05$, at Fp1 and F4), and gamma band ($P < 0.05$, at F3).

Coherence Analysis Time-Locked to Slow Oscillation. The number and magnitude of differences in EEG coherence between the learning and nonlearning conditions markedly increased when the analysis was focused on the depolarizing positive-going phase of the slow oscillation. In this positive-going phase 0–1 sec after the peak of the negative half-waves, coherence was distinctly higher after learning than nonlearning in the slow-oscillatory band (stage 2 sleep, 37 vs. 0 electrode pairs, $P < 0.001$; SWS, 16 vs. 2, $P < 0.001$), in the delta band (stage 2 sleep, 26 vs. 1, $P < 0.001$; SWS, 24 vs. 2, $P < 0.001$), and in the slow-spindle band (SWS, 11 vs. 2, $P < 0.025$). Separate analysis of the −1- to 0-sec interval before the peak of the negative half-waves, did not reveal any further consistent difference in EEG coherence between the learning conditions.

Notably, these effects on coherence in the positive-going interval

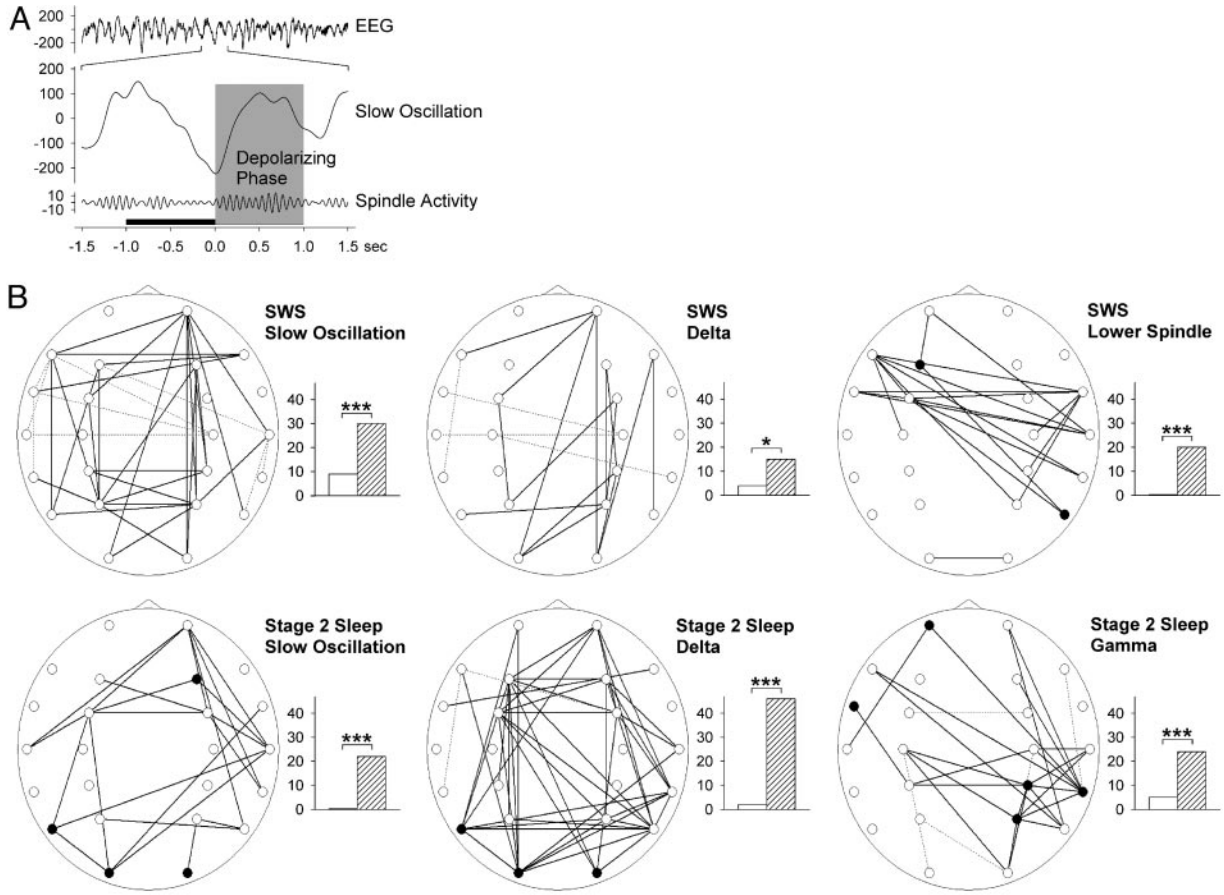

Fig. 2. Coherence analysis time-locked to slow oscillation. (*A*) Traces exemplifying extraction of slow oscillation (middle trace) and spindle activity (bottom trace) from sleep EEG (upper trace) in a single subject. Shaded area, the depolarizing positive-going phase of the slow oscillation; black bar, the preceding −1- to 0-sec interval used in some analyses as reference. (*B*) Coherence maps for slow oscillatory (*Left*), delta (*Center*), lower spindle (*Right Lower*), and gamma (*Right Lower*) bands during the positive-going phase of slow oscillation (time-locked to the negative peak of slow oscillation and adjusted to the preceding 1-sec interval). Maps indicate results for the entire subject sample ($n = 13$). Significant coherence differences ($P < 0.05$) were marked with solid lines for higher coherence during the learning condition and dashed lines for higher coherence during the nonlearning condition. In addition, electrode sites are indicated at which power on the learning condition was significantly ($P < 0.05$) higher (●) or lower (which never happened) in comparison with the nonlearning condition. Bar diagrams indicate total number of greater coherences in the learning (hatched bars) and nonlearning (white bars) condition. ***, $P < 0.001$; *, $P < 0.05$.

of the slow oscillation proved to be robust in an analysis where coherence values of the preceding −1- to 0-sec interval were subtracted from those of the 0- to 1-sec positive-going interval (Fig. 2). In this analysis, again coherence was distinctly greater after learning than nonlearning in the slow-oscillation band (stage 2 sleep, 22 vs. 0, $P < 0.001$; SWS, 30 vs. 9, $P < 0.001$) and delta band (stage 2 sleep, 46 vs. 2, $P < 0.001$; SWS, 15 vs. 4, $P < 0.025$). Also, a markedly greater coherence after learning than nonlearning was found for the slow-spindle band, although this effect appeared to be limited to SWS (20 vs. 0, $P < 0.001$). In addition, this analysis indicated enhanced coherences associated with prior learning in the beta (12 vs. 0, $P < 0.01$) and gamma (24 vs. 5, $P < 0.001$) frequency bands during stage 2 sleep.

To control for effects unrelated to a grouping by the slow oscillation, a further analysis concentrated on 1-sec intervals that were randomly distributed over the cycle of the slow oscillation. Again, coherence values of these randomly distributed 1-sec intervals were expressed as difference with reference to their respectively preceding 1-sec interval. There was no difference in EEG coherence between the learning conditions in this analysis, further supporting the time-locked nature of the differences in coherence emerging during the positive-going interval of the slow oscillation.

We also examined whether learning-induced changes in EEG coherence during slow oscillations were accompanied by systematic changes in local power. Overall, this analysis revealed local power increases after learning at some few electrode sites, contributing to the coherence changes, mainly during stage 2 sleep in the gamma band (Fp1, FT7, CP4, P4, and TP8, $P < 0.05$), the slow-oscillation band (F4, T5, O1, and O2, $P < 0.05$), and the delta band (T5, O1, and O2, $P < 0.05$). During SWS, learning-related increases in power occurred in the slow-spindle band at two locations, only (F3 and T6, $P < 0.05$; refer to Fig. 2 for a summary of respective results).

Discussion

Our data indicate that EEG coherence is enhanced during sleep after intense associative learning of word pairs, as compared with a nonlearning control condition. Importantly, this enhancement was most pronounced during the depolarizing positive-going half-wave of slow oscillations (dominant frequency of <1 Hz). During this positive-going phase, prior learning led to a strong and most robust increase in the number of recording sites showing coherent EEG activity in the slow-oscillatory, delta, lower-spindle, and gamma frequency bands. In contrast to the analysis focusing on periods time-locked to slow oscillations, effects of learning on EEG coherence were marginal in global analyses of EEG recordings during non-REM sleep. These findings suggest the slow oscillation may be of particular func-

tional significance for a reprocessing of newly acquired associations during SWS (29).

Analysis of the waking EEG during task performance indicated a distinct enhancement in EEG coherence in a wide variety of frequencies during explicit learning of the word pairs as compared with the nonlearning situation. This finding confirms a number of previous studies which, mainly based on analysis of event-related EEG activity, consistently showed similar increases in EEG coherence in tasks, such as object recognition and short-term retention tasks, demanding the explicit (i.e., declarative) encoding of representations (20, 23, 30). Weiss and Rappelsberger (23) found that the encoding of words that could be correctly recalled later was associated with enhanced coherence within all frequency bands (1–18 Hz) except the lower alpha band (8–10 Hz) in comparison with encoding of words later forgotten. This finding fits remarkably well with the present results where EEG coherence during word-pair learning was enhanced in the delta, theta, upper alpha, and beta bands, but not in the lower alpha band. Collectively, these data corroborate the concept that efficient declarative encoding of associations is bound to a large-scale synchrony of cortical neuronal activity that is sensitively reflected by EEG coherence. The frequencies involved are assumed to depend at least in part on the type and complexity of the task and to what extent local or distant cortical and subcortical networks need to be integrated for the encoding process (20, 31).

High coherence between EEG signals from different sites of the scalp hints at an increased interplay between the underlying neuronal networks. Volume conduction as an artificial source of coherence can be excluded here because it would have preferentially enhanced coherences between closer electrode sites (32). However, many of the coherences found here during sleep and during learning before sleep involved electrode pairs 12 cm and more apart. Most important, the volume conductance effect would not be expected to differentially affect sleep after learning and nonlearning. On the other hand, it is very unlikely that the distinct increase in EEG coherence during sleep after learning that we observed for the slow-oscillation, delta, and spindle bands reflects a direct cortico-cortical interaction between the different neocortical regions. Because the generation of these oscillations relies on a reciprocal interaction within thalamocortical feedback loops, it can be assumed that the same thalamocortical connections also contribute to the increase in coherence in these bands (15, 16, 29, 33).

Slow oscillations, which were originally discovered by Steriade *et al.* (15, 16) using intracellular recordings and were subsequently confirmed in human sleep EEG recordings (17, 34, 35), grasp the entire thalamocortical system. However, they can be recorded also in isolated slabs of neocortical tissue which, hence, is considered the primary generator structure of these oscillations. The negative half-wave of the slow oscillation in the human sleep EEG corresponds to a depth-positive neocortical field potential, which is associated with widespread intracellular hyperpolarization (17, 36). On the other hand, the positive half-wave marks a depth-negative extracellular field potential, reflecting widespread cortical depolarization. The hyperpolarized "down" state of slow oscillations has been shown to be linked to a general disfacilitation, rather than inhibition, of cortical networks associated with a silencing of excitatory as well inhibitory neurons, which probably results from activation of intrinsic potassium currents (37). Slow oscillations, thus, exert a fundamental temporal grouping effect on fast brain oscillations in the spindle, beta, and gamma bands. Whereas during the down state (EEG-negative half-wave) this activity is suppressed, the depolarizing up state (EEG-positive half-wave) is associated with high levels of spiking in neocortical pyramidal cells that drive through corticothalamic fibers, the thalamic generation of spindle activity spreading back to the neocortex (38, 39). Accordingly, the positive half-wave of slow oscillation is accompanied by a pronounced rebound of spindle activity (17). The close coupling of the generating mechanisms makes plausible here that, during SWS after learning, combined increases in EEG coherence accompanying slow-oscillation positivity were found to be most robust in just these two frequency bands, i.e., the slow-oscillatory and (lower) spindle-frequency bands. Analysis of multisite local field potentials in cats revealed that coherence of spindle activity was highest during states of increased cortical excitability, indicating that the depolarizing phase of the slow oscillation indeed helps to shape the large-scale in-phase synchrony of cortical spindle activity (33).

Notably, effects of learning on EEG coherence during sleep were distinctly more pronounced than and only loosely related to changes in EEG power in the respective frequency bands. Regarding power, the most consistent change was a learning-induced increase in upper spindle power. Whereas this increase is in line with previous observations of an enhanced occurrence of discrete spindles after declarative learning in humans (14, 40), it was largely unrelated to changes in coherence.

The increase in EEG coherence among widely distributed regions might in part reflect the complexity of the task, for which the subject, beyond rote learning of the written word pairs, adhered to a certain mnemonic strategy to visually imagine the word content, thereby relying on an integration of verbal, visual, and spatial cortical functions. Previous studies (41–43) indicated a particular involvement of left frontotemporal and right parietal cortical regions in the encoding of word pairs. In support of these findings, here coherence during learning before sleep was distinctly enhanced between left frontal and right parietal areas in the upper alpha band (10–13 Hz, Fig. 1). However, increased EEG coherences found during learning in the delta, theta, and beta bands indicated an involvement also of further regions, such as the right frontal and left parietotemporal regions during performance on the learning task. Interestingly, the pattern of increased coherences in the upper alpha band between left frontal and right parietal regions seen during learning before sleep, shared some similarity with the distribution of slow-oscillation-bound coherences in the (lower) spindle and gamma bands during subsequent sleep suggesting that these interhemispheric connections became partly reactivated. This observation would fit the concept that the same cell assemblies activated during encoding interact more strongly than others during subsequent SWS. Nevertheless, one should be cautioned against taking the observed EEG changes as direct reflection of an actual reprocessing of the representations acquired before sleep. Our learning task activated a variety of cortical regions and was not designed to invoke activity in a select cortical region. Thus, conclusions regarding the topography of EEG coherence remain tentative. In the same way, it could be argued that the EEG frequencies indicating coherence changes at learning are different from those whose coherence changed in sleep after learning. However, this result might not be surprising, considering that the entire sleep EEG differs in the predominant frequencies from the waking EEG, especially during SWS. Data corroborating the view that slow oscillations could be involved in a reprocessing of newly acquired representations come from a recent study (44) indicating a local increase in slow-wave activity during sleep after learning specifically in areas involved in task acquisition, with this increase being correlated with later retrieval performance.

Our data indicate an experience-dependent increase of EEG coherence during sleep after a period of intense declarative learning, which is not necessarily related to any memory function of sleep (45). However, in identifying the depolarizing positive-going phase of slow oscillations as a time period associated with a striking increase in learning-dependent EEG coherence, the results fit well with recent concepts connecting slow oscillations to iterative processes of memory formation during SWS (29, 46, 47). According to these models, the long-range synchrony in

cortical activity associated with the up state (surface positivity) of slow oscillations drives thalamocortical spindle activity, which is associated with a massive calcium entry into cortical pyramidal cells. It thereby sets the stage for synaptic plastic changes in these cells through activation of calcium-dependent kinases. Concurrently, the strong synchronous cortical excitation associated with the slow oscillation up state is thought to trigger hippocampal ripple activity, a mechanism underlying the transfer of information encoded in hippocampal populations to neocortical networks (12, 13, 48). Coincident inputs from spindle and ripple activity to cortical populations could in this way set the stage for plastic processes in specific neocortical representations.

According to the outlined concept, the depolarizing positive phase of slow oscillations enables plastic processes in specific neocortical networks by synchronizing thalamic and hippocampal inputs. On this background, an intriguing question pertains to the mechanism initiating this depolarizing up state, which seemingly emerges from a period of neuronal silence (29). Interestingly, as one mechanism initiating positivity, miniature excitatory postsynaptic potentials have been identified. They randomly summate during the down state of slow oscillations and may act in concert with slow hyperpolarization-activated cation currents to depolarize cortical pyramidal cells above threshold (49). Assuming that the probability of miniature excitatory postsynaptic potentials during the silent down phase is selectively enhanced at synapses previously activated during associative learning (50–53), this ongoing miniature activity could well explain the present observation of increased coherence of slow oscillations between cortical regions previously engaged in the learning process.

We thank Auja Otterbein for organizational work. This study was supported by Deutsche Forschungsgemeinschaft Grant FOR 457.

1. McGaugh, J. L. (2000) *Science* **287,** 248–251.
2. Müller, G. E. & Pilzecker, A. (1900) *Z. Psychol.*, Suppl. 1, 1–300.
3. McNaughton, B. L., Barnes, C. A., Battaglia, F. P., Bower, M. R., Cowen, S. L., Ekstrom, A. D., Gerrard, J. L., Hoffman, K. L., Houston, F. P., Karten, Y. *et al.* (2003) in *Sleep and Brain Plasticity*, eds. Maquet, P., Smith, C. & Stickgold, R. (Oxford Univ. Press, New York), pp. 225–246.
4. Maquet, P. (2001) *Science* **294,** 1048–1052.
5. Stickgold, R., Hobson, J. A., Fosse, R. & Fosse, M. (2001) *Science* **294,** 1052–1057.
6. Pavlides, C. & Winson, J. (1989) *J. Neurosci.* **9,** 2907–2918.
7. Wilson, M. A. & McNaughton, B. L. (1994) *Science* **265,** 676–679.
8. Kudrimoti, H. S., Barnes, C. A. & McNaughton, B. L. (1999) *J. Neurosci.* **19,** 4090–4101.
9. Buzsáki, G. (1996) *Cereb. Cortex* **6,** 81–92.
10. McClelland, J. L., McNaughton, B. L. & O'Reilly, R. C. (1995) *Psychol. Rev.* **102,** 419–457.
11. Qin, Y. L., McNaughton, B. L., Skaggs, W. E. & Barnes, C. A. (1997) *Philos. Trans. R. Soc. London B* **352,** 1525–1533.
12. Siapas, A. G. & Wilson, M. A. (1998) *Neuron* **21,** 1123–1128.
13. Sirota, A., Csicsvari, J., Buhl, D. & Buzsáki, G. (2003) *Proc. Natl. Acad. Sci. USA* **100,** 2065–2069.
14. Gais, S., Mölle, M., Helms, K. & Born, J. (2002) *J. Neurosci.* **22,** 6830–6834.
15. Steriade, M., Nuñez, A. & Amzica, F. (1993) *J. Neurosci.* **13,** 3252–3265.
16. Steriade, M., Nuñez, A. & Amzica, F. (1993) *J. Neurosci.* **13,** 3266–3283.
17. Mölle, M., Marshall, L., Gais, S. & Born, J. (2002) *J. Neurosci.* **22,** 10941–10947.
18. Singer, W. (1993) *Annu. Rev. Physiol.* **55,** 349–374.
19. König, P. & Engel, A. K. (1995) *Curr. Opin. Neurobiol.* **5,** 511–519.
20. von Stein, A., Rappelsberger, P., Sarnthein, J. & Petsche, H. (1999) *Cereb. Cortex* **9,** 137–150.
21. John, E. R. (2002) *Brain Res. Rev.* **39,** 1–28.
22. Miltner, W. H., Braun, C., Arnold, M., Witte, H. & Taub, E. (1999) *Nature* **397,** 434–436.
23. Weiss, S. & Rappelsberger, P. (2000) *Brain Res.* **9,** 299–312.
24. Plihal, W. & Born, J. (1997) *J. Cognit. Neurosci.* **9,** 534–547.
25. Gais, S. & Born, J. (2004) *Proc. Natl. Acad. Sci. USA* **101,** 2140–2144.
26. Rechtschaffen, A. & Kales, A. (1968) *A Manual of Standardized Terminology, Techniques, and Scoring System for Sleep Stages of Human Subjects* (U.S. Dept. of Health, Education, and Welfare, Bethesda).
27. De Gennaro, L. & Ferrara, M. (2003) *Sleep Med. Rev.* **7,** 423–440.
28. Gratton, G., Coles, M. G. & Donchin, E. (1983) *Electroencephalogr. Clin. Neurophysiol.* **55,** 468–484.
29. Steriade, M. & Timofeev, I. (2003) *Neuron* **37,** 563–576.
30. Mima, T., Oluwatimilehin, T., Hiraoka, T. & Hallett, M. (2001) *J. Neurosci.* **21,** 3942–3948.
31. Varela, F., Lachaux, J. P., Rodriguez, E. & Martinerie, J. (2001) *Nat. Rev. Neurosci.* **2,** 229–239.
32. Srinivasan, R., Nuñez, A. & Silberstein, R. B. (1998) *IEEE Trans. Biomed. Eng.* **45,** 814–826.
33. Destexhe, A., Contreras, D. & Steriade, M. (1999) *J. Neurosci.* **19,** 4595–4608.
34. Achermann, P. & Borbély, A. A. (1997) *Neuroscience* **81,** 213–222.
35. Marshall, L., Mölle, M., Fehm, H. L. & Born, J. (2000) *Eur. J. Neurosci.* **12,** 3935–3943.
36. Steriade, M., Contreras, D. & Amzica, F. (1994) *Trends Neurosci.* **17,** 199–208.
37. Timofeev, I., Grenier, F. & Steriade, M. (2001) *Proc. Natl. Acad. Sci. USA* **98,** 1924–1929.
38. Contreras, D. & Steriade, M. (1995) *J. Neurosci.* **15,** 604–622.
39. Destexhe, A., Contreras, D. & Steriade, M. (1999) *Neuroscience* **92,** 427–443.
40. Meier-Koll, A., Bussmann, B., Schmidt, C. & Neuschwander, D. (1999) *Percept. Mot. Skills* **88,** 1141–1159.
41. Grady, C. L., McIntosh, A. R., Rajah, M. N. & Craik, F. I. (1998) *Proc. Natl. Acad. Sci. USA* **95,** 2703–2708.
42. Cabeza, R. & Nyberg, L. (2000) *Curr. Opin. Neurol.* **13,** 415–421.
43. Mölle, M., Marshall, L., Fehm, H. L. & Born, J. (2002) *Eur. J. Neurosci.* **15,** 923–928.
44. Huber, R., Ghilardi, M. F., Massimini, M. & Tononi, G. (2004) *Nature* **430,** 78–81.
45. Cantero, J. L., Atienza, M., Salas, R. M. & Dominguez-Marin, E. (2002) *J. Neurosci.* **22,** 4702–4708.
46. Sejnowski, T. J. & Destexhe, A. (2000) *Brain Res.* **886,** 208–223.
47. Buzsáki, G. (1998) *J. Sleep Res.* **7,** Suppl. 1, 17–23.
48. Nadasdy, Z., Hirase, H., Czurko, A., Csicsvari, J. & Buzsaki, G. (1999) *J. Neurosci.* **19,** 9497–9507.
49. Bazhenov, M., Timofeev, I., Steriade, M. & Sejnowski, T. J. (2002) *J. Neurosci.* **22,** 8691–8704.
50. Oliet, S. H., Malenka, R. C. & Nicoll, R. A. (1996) *Science* **271,** 1294–1297.
51. Bao, J. X., Kandel, E. R. & Hawkins, R. D. (1998) *J. Neurosci.* **18,** 458–466.
52. Hoffman, K. L. & McNaughton, B. L. (2002) *Science* **297,** 2070–2073.
53. Eliot, L. S., Kandel, E. R. & Hawkins, R. D. (1994) *J. Neurosci.* **14,** 3280–3292.